NASA TM-85703

NASA Technical Memorandum 85703

PREDICTION OF IMPACT FORCE AND DURATION DURING LOW VELOCITY IMPACT ON CIRCULAR COMPOSITE LAMINATES

K. N. Shivakumar, W. Elber, and W. Illg

October 1983

NASA
National Aeronautics and Space Administration

Langley Research Center
Hampton, Virginia 23665

PREDICTION OF IMPACT FORCE AND DURATION DURING LOW VELOCITY IMPACT ON CIRCULAR COMPOSITE LAMINATES

K. N. Shivakumar,* W. Elber,** and W. Illg**
NASA Langley Research Center
Hampton, VA 23665

SUMMARY

Two simple and improved models - energy-balance and spring-mass - were developed to calculate impact force and duration during low-velocity impact of circular composite plates. Both models include the contact deformation of the plate and the impactor as well as bending, transverse shear, and membrane deformations of the plate. The plate was a transversely isotropic graphite/epoxy composite laminate and the impactor was a steel sphere.

In the energy-balance model, a balance equation was derived by equating the kinetic energy of the impactor to the sum of the strain energies due to contact, bending, transverse shear, and membrane deformations at maximum deflection. The resulting equation was solved using the Newton-Raphson numerical technique. The simple energy-balance model, yields only the maximum force; hence a less simple spring-mass model is presented to calculate the force history.

In the spring-mass model, the impactor and the plate were represented by two rigid masses and their deformations were represented by springs. Springs define the elastic contact and plate deformation characteristics. Equations of equilibrium of the resulting two degree-of-freedom system, subjected to an initial velocity, were obtained from Newton's second law of motion. The two coupled nonlinear differential equations were solved using Adam's numerical integration technique. Calculated impact forces from the two analyses agreed with each other. The analyses were verified by comparing the results with reported test data.

---

*Research Associate Professor, Old Dominion University
**Senior Engineer

INTRODUCTION

Low-velocity impact of composite laminates has been a subject of importance since the last decade. The invisible damage caused by mild impacts was found to decrease residual strengths. Many researchers have studied this problem in different ways. Yet the problem still poses many challenges. Methods reported [1-8] to date to predict the impact force, including the effect of contact deformation, can be classified into two categories: (1) the Hertz method; and (2) the modified Hertz method. The Hertz method, which includes only the contact deformation for plates supported at the outer boundary, overestimates impact force by several orders of magnitude [3]. The modified Hertz method includes the plate flexural deflection in addition to contact deformation. Impact of rectangular [5,6,7], circular [4], and cantiliever [3] plates was studied based on small deflection thin plate theory. Recent studies [8,9], however, have shown that the laminates (plates) undergo large deflection and transverse shear deformation when the impact occurs at low velocity. The modified Hertz method [3-7], which neglects these two effects, underestimates the impact force for thin plates and overestimates the force for thick plates. Hence, it is necessary to develop a more general analysis that includes both large deflection and transverse shear effects, so that a wider range of plate thickness and impact velocities could be analyzed accurately. An exact solution for the low-velocity impact on composite laminates involves a three-dimensional nonlinear dynamic analysis of a laminate attached to a central mass through a Hertzian spring. Such an analysis is mathematically highly complex and numerically intractable even with modern computers. The objective of this paper is, therefore, to develop improved, yet simple, analyses to calculate the impact force and duration for a low-velocity impact on circular laminates.

The particular problem considered in this study was a circular laminated plate impacted at its center by a stiff sphere. The plate was assumed to be made up of a quasi-isotropic laminate having transversely isotropic material properties. The plate boundary was either clamped or simply supported. During impact, the plate and the impactor undergo contact deformation and the plate further undergoes bending, transverse shear and membrane deformations. Early studies [1,8,10] have shown that the impact duration is many times longer than the time for generated stress waves to travel to the outer boundary of the plate and to return. Furthermore, the effects of higher modes, especially when the plate undergoes large deflection, are small and can be neglected. Therefore, assuming the first mode vibration of the plate, two simple models were proposed: (1) an energy-balance model and (2) a spring-mass model. The energy-balance model (equating the kinetic energy of the impactor before the impact to the deformation energies of the plate-impactor system) yielded an energy equation which could be solved for maximum force using a desk top calculator. However, to calculate the complete force history during impact, the spring-mass model was developed. In the spring-mass model, the impactor and the plate were represented by two rigid masses and the associated deformation characteristics were represented by springs. Equations of motion of the two masses were obtained using Newton's second law of motion. The resulting coupled nonlinear differential equations then were solved using Adam's numerical integration technique. The two analyses were compared with each other and with reported data [4,9].

SYMBOLS

a	plate radius, m
a_c	contact radius, m
A_{11}, A_{12}, A_{22}	contact stiffness constants
E	Young's modulus, MPa
E_c	contact deformation energy, N-m
E_m	membrane deformation energy, N-m
E_{bs}	bending-shear deformation energy, N-m
G	shear modulus, MPa
h	plate thickness, m
K_b	plate bending stiffness, N/m
K_m	plate membrane stiffness parameter, N/m
K_s	plate shear stiffness, N/m
K_{bs}	equivalent bending-shear stiffness, N/m
K_1, K_2	constants
M	mass, kg
n	contact deformation stiffness
P	impact force, N
R_I	impactor radius, m
r-z	plate coordinate system
t	time, seconds
V_o	impact velocity, m/sec
w	plate total transverse deflection at the center, m
w_b	plate bending deflection, m
w_s	plate transverse shear deflection, m
x_1	impactor displacement response, m
x_2	plate displacement response, m

α contact deformation of impactor and plate, m

β, δ contact stiffness constants

ν Poisson's ratio

ρ material density, kg/m^3

Subscripts:

I impactor

p plate

r radial direction

z transverse direction

DESCRIPTION OF THE PROBLEM

Figure 1 (top) shows a spherical impactor of radius R_I, mass M_I, and velocity V_o striking the center of a circular plate of radius a and thickness h. The plate is assumed to be made up of a quasi-isotropic laminate having transversely isotropic material properties. A cylindrical coordinate system with the origin at the center of the plate is assumed. A representative θ = constant section of the plate is shown in the Figure 1. During impact ($t > 0$), the impact force induces two types of deformations [4]: (1) contact deformation α in the impactor and the plate (see fig. 1), and (2) transverse deflection w of the plate, which is measured from its mid-surface (see fig. 1). The deformation α is the measure of how the centers of the plate and the impactor approach each other. The impact force P and the contact deformation are related by the well-known Hertz law [2,11]. The transverse deflection w is the sum of bending w_b and transverse shear w_s deformations of the plate. (From hereon "transverse shear" is referred to as 'shear.') Furthermore, the membrane deformation is caused by the stretching associated with the deflection w of the plate. If w is small compared to plate thickness ($w/h \leq 0.2$), the membrane effects could be neglected [12].

After the plate-impactor contact, the impact force P (see fig. 1) acts over an area of contact between the impactor and the plate. The area of contact depends on the force and moduli of the impactor and plate. The plate load and deflection are related by the stiffness associated with bending, shear and membrane deformations. Because the area of contact is small, it was assumed that the impact force was centrally concentrated. The expressions for bending stiffness K_b and membrane stiffness K_m parameters were derived using the Babunov-Galerkin variational method [13]. These stiffness expressions for K_b and K_m are given in Table 1 for the four plate boundaries, namely, clamped (edge moveable or immoveable) and simple supported (edge moveable or immoveable). The transverse shear stiffness K_s expression was derived assuming the impact force to be distributed over the region of contact [14]. This K_s expression was verified by comparing the calculated shear deformation with Woinowsky-Krieger's [12] results for isotropic plates. The formulation and results of the proposed two models, energy-balance model and spring-mass model, are presented in the following sections.

ENERGY-BALANCE MODEL

Analysis

The energy-balance (E-B) model was based on the principle of conservation of total energy of the plate-impactor system In this analysis, the kinetic energy of the impacting mass was equated to the sum of the energies due to contact, bending, shear, and membrane deformations. The energy losses from material damping, surface friction, and higher mode vibrations [10] were neglected. The resulting equation was solved for the impact force using the standard Newton-Raphson numerical technique.

The maximum kinetic energy of the impactor before impact, at $t = o$, is $1/2\ M_I V_o^2$. After $t = o$, the plate-impactor system undergoes contact,

bending-shear, and membrane deformations. The corresponding stored deformation energies are E_c, E_{bs}, and E_m, respectively. Then, from the principle of conservation of total energy, the energy-balance equation of the plate-impactor system is

$$\frac{1}{2} M_I V_o^2 = E_c + E_{bs} + E_m \tag{1}$$

The energies E_c, E_{bs}, and E_m were calculated using the corresponding force-deformation relations as follows.

The impact force P and contact deformation α relation for impact of two bodies of revolution is given by the Hertz law [2],

$$P = n\alpha^{3/2} \tag{2}$$

where n is the contact stiffness parameter, which depends on material and geometrical properties of the plate and the impactor. The expression for n, for an isotropic impactor and transversely isotropic composite plate, is given by [11]

$$n = \frac{4\sqrt{R_I}}{3\pi(K_1 + K_2)} \tag{3}$$

where

$$K_1 = \left(\frac{1 - \nu_I^2}{\pi E_I} \right)$$

and

$$K_2 = \frac{\sqrt{A_{22}}\left[\left(\sqrt{A_{11}A_{22}} + G_{zr}\right)^2 - \left(A_{12} + G_{zr}\right)^2\right]^{1/2}}{2\pi\sqrt{G_{zr}}\left(A_{11}A_{22} - A_{12}^2\right)}$$

$$A_{11} = E_z(1 - \nu_r)\beta$$

$$A_{22} = \frac{E_r\beta(1 - \nu_{zr}^2\delta)}{(1 + \nu_r)}$$

$$A_{12} = E_r\nu_{zr}\beta$$

$$\beta = \frac{1}{1 - \nu_r - 2\nu_{zr}^2\delta}$$

$$\delta = E_r/E_z$$

The constants E_I and ν_I are, respectively, Young's modulus and Poisson's ratio of the impactor. The constants E, G, and ν are, respectively, Young's modulus, shear modulus, and Poisson's ratio of the plate, while the subscripts r and z refer to radial and thickness directions, respectively.

The contact energy E_c is then the integral of the product of the impact force and contact deformation:

$$E_c = \int_0^{\alpha} P \, d\alpha$$

The impact force P is replaced by the function α from equation (2), then after integration and simplification E_c becomes

$$E_c = \frac{2}{5} \frac{P^{5/3}}{n^{2/3}} \tag{4}$$

The reactive force P from the plate can be resolved into two components

$$P = P_{bs} + P_m \tag{5}$$

where P_{bs} is the force associated with bending and shear deformations and the P_m is the force associated with membrane deformation. Using the force-deflection relation reported in reference 13, the force P is written as

$$P = K_{bs}w + K_m w^3 \tag{6}$$

where $K_{bs} = \frac{K_b K_s}{K_b + K_s}$ is the effective stiffness due to bending and shear. The constants K_b, K_s, and K_m are bending, shear, and membrane stiffnesses, respectively, of the target. Expressions for K_b and K_m for the four plate boundary conditions are given in Table 1. The shear stiffness K_s was derived starting from the shear stress-strain relation for transverse loading of a circular target [14]. It is given by

$$K_s = \frac{4\pi G_{zr} h}{3} \left(\frac{E_r}{E_r - 4\nu_{rz} G_{zr}} \right) \left(\frac{1}{4/3 + \log a/a_c} \right) \tag{7}$$

The contact radius a_c is the radius of contact between the impactor and the target, which depend on the force P, and which is expressed as [4]

$$a_c = \left[\frac{3\pi}{4} P(K_1 + K_2) R_I \right]^{1/3} \tag{8}$$

The impact force P is initially unknown, hence an initial value of $a_c = h/2$ was used in equation (7) for the estimation of P. the bending-shear energy E_{bs}, and membrane energy E_m of the target, were obtained by integrating the forces P_{bs} and P_m (from equations (5) and (6)) with respect to w. Therefore,

$$E_{bs} = \frac{1}{2} K_{bs} w^2 \tag{9}$$

and

$$E_m = \frac{1}{4} K_m w^4 \tag{10}$$

Substituting equations (4), (9), and (10) in equation (1), and then simplifying using equation (6), the energy-balance equation becomes

$$M_I V_o^2 = K_{bs} w^2 + \frac{K_m w^4}{2} + \frac{4}{5}\left[\frac{\left(K_{bs} w + K_m w^3\right)^5}{n^2}\right]^{1/3} \tag{11}$$

The deflection w is calculated solving equation (11), using the Newton-Raphson numerical technique. The inverse procedure of calculating the impact velocity for a chosen value of w can also be followed. The impact force P is then calculated by substituting the value of w into equation (6). The analysis was repeated for different plate configurations and impact velocities. Typical results for the E-B model are presented in the next section.

Results

The impactor was a steel sphere of radius 19 mm, and the plate was a quasi-isotropic graphite/epoxy laminate of radius 38 mm. Material properties

of the impactor and the laminate used in the analysis and given in Table 2. Clamped and simply-supported plate boundaries were examined.

Figure 2 shows impact force versus impact velocity for three different plate thicknesses: 3.2, 1.6, and 0.8 mm for a plate radius of 38 mm. The plate boundary was clamped and edge immoveable. The case of $h = 3.2$ mm ($a/h = 12$) was a moderately thick plate, wherein the transverse shear deformation is significant, and $h = 0.8$ mm was a thin plate wherein the membrane stretching is large. The solid lines represent the E-B model results and the broken lines represent Greszczuk's [4] results, in which both large deflection and shear deformation effects were neglected. The two analyses agree over only limited velocity ranges, depending on the plate thickness. The E-B model predicts lower impact force for thick plates ($h = 3.2$ mm) than Greszczuk's analysis due to transverse shear flexibility (plate deflections were in the small deflection range). At higher velocities, the plate deflection becomes larger and the associated membrane stiffening counteracts shear flexibility; hence, the two results approach each other before crossing at $V_o = 8.5$ m/sec. For thin plates, the two analyses agree only at very low velocities (less than 1 m/sec, which is not of practical interest); at higher velocities the E-B model predicts higher impact force than the Greszczuk, due to membrane stiffening.

Figure 3 shows the variation of contact deformation energy with impact velocity for the same plates The contact energy is normalized with respect to the kinetic energy of the impactor, i.e., $E_c/(1/2\ M_I V_o^2)$. As before, solid lines represent the E-B model results and broken lines represent the Greszczuk analysis. The E-B model results show that the contact deformation energy initially decreases with increase in impact velocity, and finally increases at higher velocities, whereas Greszczuk's analysis shows a monotonic

decrease in contact energy. This difference is due to neglecting the effect of large deflection (membrane stiffening) in the Greszczuk's analysis. But the two results agree very well for thin targets at very low impact velocities (a region of academic interest). Examining the contact energy for thin plates in figure 3, one can conclude that contact effects may be neglected for very thin plates.

Figure 4 shows maximum impact force versus velocity for the same plates but with simply-supported edges (roller supports). The E-B model and the Greszczuk analysis agree well for h = 3.2 mm, due to the counteracting effect of membrane stiffening and the transverse shear flexibility in the plate. Furthermore, the two analyses agree for thin plates at very low velocities. But at higher velocities, the E-B model predicts higher impact force than the Greszczuk analysis. Comparison of results from figures 3 and 5 show that for a given impact velocity, the clamped plate (due to higher bending and membrane stiffness) experiences higher impact force than the simply-supported plate.

Figure 5 compares the predicted and measured [4] impact forces for a simply-supported plate of radius 38 mm and thickness of 36 mm. Notice that the ordinate scales in figure 5 are linear, whereas in figure 5 they were logarithmic. Calculated impact forces are represented by curves, and the test results [4] by symbols. The broken line (— — —) is from the spring-mass model, which will be explained in the next section. Results from the E-B model agree well with test data at low velocities, and reasonably well at higher velocities. The discrepancy may be due to plate damage during the impact (P = 1.6 KN, V_o = 2.54 m/sec). However, predictions from the present E-B model are closer to test data than are Greszczuk's predictions.

SPRING-MASS MODEL

Analysis

The energy-balance model presented in the previous section estimates the impact force fairly accurately. But it does not predict the history of force, velocity or displacement throughout the impact. So an alternate model, namely a "spring-mass" model (S-M model), is presented here. The S-M model is an extension of Lee's spring-mass model for impact of beams [1]. In the present S-M model (fig. 6), the impactor and the plate were represented by two rigid mases M_I and M_p, respectively. The early studies [15] on free vibrations of plates with an attached central concentrated mass have indicated that the effective mass of the plate contributing to inertial effects is one-fourth of its total mass. Hence, in the present analysis also, the effective plate mass M_p was taken as one-fourth of the total mass of the plate. The two masses were connected through a Hertzian spring that represented the contact load-deformation characteristics [11]. The transverse load-deformation behavior of the plate was represented by a combination of bending, shear, and membrane springs (see fig. 6(a)). The spring combination below the plate mass satisfy the following conditions: impact force is shared by bending shear and membrane deformations of the plate; for thin plates the spring combination reduces to the thin plate theory due to relatively low bending stiffness $\left(K_{bs} = \frac{1}{1/K_b + 1/K_s} \approx K_b\right)$; for small plate deflections ($w < 0.2\ h$), the spring combination reduces to the small deflection theory due to relatively small force carried by membrane stretching ($P = K_m w^3$). Bending and membrane stiffness expressions for four types of plate boundaries are given in Table 1; the shear stiffness expression is given by equation (7). Again, material damping, plate damage, and surface friction were neglected.

Let $x_1(t)$ and $x_2(t)$ (see fig. 6(a)) represent the displacement responses of the two masses at any time t after impact. The corresponding velocities were represented by $\dot{x}_1(t)$ and $\dot{x}_2(t)$. The dot indicates the differentiation with respect to time t. The transverse deflection of the plate is given by $w = x_2(t)$ and the contact deformation is given by $\alpha = x_1(t) - x_2(t)$. Throughout the analysis the impactor mass M_I was assumed to be in contact with the plate. Applying Newton's second law of motion, equations of equilibrium of the two degree-of-freedom (TDOF) spring-mass systems are written as (see fig. 2(b))

$$M_I\ddot{x}_1 + \lambda n\left|(x_1 - x_2)\right|^{1.5} = 0 \tag{12}$$

$$M_p\ddot{x}_2 + K_{bs}x_2 + K_m x_2^3 - \lambda n\left|(x_1 - x_2)\right|^{1.5} = 0 \tag{13}$$

and

$$\lambda = 1 \quad \text{for} \quad x_1 > x_2$$

$$\lambda = -1 \quad \text{for} \quad x_1 < x_2$$

Initial conditions of the two masses are: $x_1(0) = 0$ and $\dot{x}_1(0) = V_o$ for the mass M_I; and $x_2(0) = \dot{x}_2(0) = 0$ for the plate mass M_p. The coupled non-linear differential equations were solved using Adam's numerical integration technique. Calculations were stopped when the plate displacement $x_2(t)$ became zero or negative. The impact force experienced by the plate was calculated by substituting $x_2(t)$ in place of w in equation (6).

If the effective plate mass M_p is less than 0.071 times the impactor mass (or impactor mass M_I is greater than 3.5 times the total plate mass), reference 15 suggested that the plate mass could be neglected. The two degree-of-freedom system then reduces to a single degree-of-freedom (SDOF) system as shown in figure 6(b). Then the equation of equilibrium of M_I is written as

$$M_I\ddot{x}_1 + K_{bs}w + K_m w^3 + n\alpha^{1.5} = 0 \tag{14}$$

and

$$x_1 = w + \alpha \tag{15}$$

Initial conditions are $t = 0$, $x_1(0) = 0$, and $\dot{x}_1(0) = V_o$. Equations (14) and (15) were solved numerically for $x_1(t)$ and P as before.

Results

Impact force and the duration due to an impact of a steel ball on a circular plate were calculated using the S-M model. Two impactor sizes 19 mm and 12.8 mm, and two types of plate materials, aluminum and graphite/epoxy, were used in the analysis. The analysis was first verified by comparing the calculated impact durations with reported test results [4] for aluminum plates. Then, impact force and the duration were calculated for graphite/epoxy laminates, and compared with reported results.

Figure 7 shows velocity, displacement, and force responses of impactor and plate when a steel ball of radius 19 mm impacted on an aluminum plate (a = 38 mm) at a velocity of 2.54 m/sec. Solid lines represent the two degree-of-freedom (TDOF) spring-mass results and broken lines represent the single degree-of-freedom (SDOF) spring-mass results. In figure 7(a), the

velocity of the impactor decreases from an initial velocity of 2.54 m/sec to zero and then to -2.54 m/sec. The incident and the rebound velocities were equal because energy losses in the system were neglected. The time elapsed during the impactor velocity excursion from +2.54 m/sec to -2.54 m/sec is defined as the impact duration. The duration was 0.607 msec from both TDOF and SDOF analyses. The perturbations in the TDOF results are due to interacting inertial forces of the two masses.

Figure 7(b) shows the displacement response of the impactor (x_1) and the plate (x_2) masses calculated from the two spring-mass models. The impactor and target displacements were zero initially and then attained maximum when the impactor velocity reached zero, before becoming zero again. In the case of the TDOF analysis, the plate displacement x_2 was higher than the impactor x_1 for a few micro-seconds in the early part and later part of the impact event. The separation of masses was not allowed, since the impactor was assumed in contact with the plate throughout the analysis. These small distrubances were due to inertial effects of the plate; inclusion of material damping would have reduced these disturbances.

Figure 7(c) shows variation of plate reaction with time. The absolute maximum reaction experienced by the plate during the impact event is defined as the impact force. The SDOF curve passes through the mean of the TDOF results. In figures 7(a) - 7(c) ($M_I/M_p = 23$), the TDOF and SDOF agree very well; hence, for large ratio of impactor mass to plate mass, the inertial effects of the plate may be neglected.

Figure 8 compares predicted and measured [4] impact durations on aluminum plates of various thicknesses. The solid line represents the TDOF S-M model results and symbols are from test data [4]. The analysis agrees reasonably well with test results. The discrepancy may be due to two main assumptions in

the analysis: the plate is perfectly elastic, whereas in the tests local plastic deformation is possible; and the boundary is perfectly clamped, whereas, actually, rubber grip pads were used in the test [4]. The figure shows that the impact duration decreases with increase in plate thickness.

Returning to figure 5, it shows the comparison of impact force calculated from spring-mass model, energy-balance model, and Greszczuk's analysis and test data [4] for simply-supported composite plates. Calculated forces from the spring-mass model and energy-balance model agree very well, and both agree with test data, except at the higher impact velocity.

Figure 9(a) shows the comparison of predicted and measured [9] impact duration for a clamped composite plate at various velocities. the plate was an 8-ply graphite/epoxy composite with quasi-isotropic laminate and 45 mm radius. The TDOF spring-mass model results agree with test data [9], except at low velocities. Calculated impact forces (fig. 9(b)) for the same configurations agree reasonably well with test data [9]. Results from the energy-balance model are also shown and are very close to the TDOF spring-mass model results.

CONCLUSIONS

Two simple and improved models, an energy-balance model and a spring-mass model, were developed to calculate impact force and duration associated with low-velocity impact on circular composite plates. Both models include the contact deformation of the plate and the impactor as well as the bending, shear, and membrane deformations of the plate. The plate materials were transversely isotropic graphite/epoxy laminate or aluminum and the impactor was a steel sphere.

The energy-balance model was based on the principle of conservation of total energy This analysis yielded a simple energy-balance equation, which

was used to calculate maximum impact force. The spring-mass model was based on the response analysis of the plate and the impactor assuming them as a combination of rigid masses and springs. The resulting equations were solved to calculate the impact force history. The analysis led to the following conclusions:

1. The energy-balance model is simple, and accurately predicts the maximum impact force; the spring-mass model, which is less simple, predicts the complete force history.
2. Impact forces calculated from the two models agreed with each other and with reported data. Also, impact durations from the spring-mass model agreed with reported test data.
3. Thin plates undergo membrane stretching and the calculated impact forces are greater than those based on small deflection theory.
4. Thick plates undergo significant transverse shear deformation that must be accounted to predict the impact force accurately.
5. When the impactor mass is greater than 3.5 times the plate mass, the inertial effects of the plate are negligible. Hence, the plate-impactor system could be represented by a single degree-of-freedom system.

REFERENCES

1. E. H. Lee, "Impact of a Mass Striking a Beam," J. Applied Mechanics, Dec. 1940, pp. 1-129 to A-138.
2. W. Goldsmith, "Impact," Edward Arnold Ltd., London, 1960.
3. J. L. Preston, Jr., and T. S. Cook, "Impact Response of Graphite/Epoxy Flat Laminates Using Projectiles That Simulate Aircraft Engine Encounters," ASTM STP568, American Society for Testing Materials, 1975, pp. 49-71.
4. L. B. Greszczuk, "Damage in Composite Materials Due to Low Velocity Impact," J. A. Zukas, et al., "Impact Dynamics," John Wiley and Sons, New York, 1982.
5. C. T. Sun and S. Chattopadhyay, "Dynamic Response of Anisotropic Plates Under Initial Stress Due to Impact of a Mass," Trans. ASME, J. Appl. Mech., Vol. 42, 1975, p. 693.
6. A. L. Dobyns and T. R. Porter, "A Study of the Structural Integrity of Graphite/Epoxy Composite Structure Subjected to Low Velocity Impact," Polymer Engineering and Science, June 1981, Vol. 21, No. 8.
7. A. L. Dobyns, "Analysis of Simply-Supported Orthotropic Plates Subjected to Static and Dynamic Loads," AIAA paper No. 80-0680, 1980.
8. W. Elber, "Failure Mechanics in Low-Velocity Impacts on Thin Composite Plates," NASA TP 2152, May 1983.
9. K. M. Lal, "Prediction of Residual Tensile Strength of Transversely Impacted Composite Laminates," Research in Structural and Solid Mechanics," NASA CP 2245, pp. 97-112.
10. Lord Rayleigh, "On the Prediction of Vibrations by Forces of Relatively Long Duration," Philosophical Magazine Series 6, Vol. 11, 1906, p. 283.
11. H. D. Conway, Z. Angew, Math and Physics, Vol. 17, 1956, p. 460.

12. S. P. Timoshenko, and S. Woinowsky-Krieger, "Theory of Plates and Shells," McGraw-Hill, New York, 1959.

13. A. S. Volmir, "A Translation of Flexible Plates and Shells," AFFDL-TR-66-216, April 1967.

14. S. A. Lukasicwiez, "Introduction of Concentrated Loads in Plates and Shells," Progress in Aerospace Science, Vol. 17, No. 2, 1976, pp. 109-146.

15. A. W. Leissa, "Vibrations of Plates," NASA SP-160, 1969.

Table 1. Bending and Membrane Stiffness Parameters of Centrally Loaded Plates

Boundary conditions	Edge conditions	Bending stiffness, K_b	Membrane stiffness parameters, K_m
Clamped*	Immovable	$\frac{4\pi E_r h^3}{3(1-\nu_r^2)a^2}$	$\frac{(353-191\nu_r)\pi E_r h}{648(1-\nu_r)a^2}$
	Movable	$\frac{4\pi E_r h^3}{3(1-\nu_r^2)a^2}$	$\frac{191\pi E_r h}{648a^2}$
Simply supported**	Immovable	$\frac{4\pi E_r h^3}{3(3+\nu_r)(1-\nu_r)a^2}$	$\frac{\pi E_r h}{(3+\nu_r)^4 a^2}\left\{\frac{191}{648}(1+\nu_r)^4+\frac{41}{27}(1+\nu_r)^3+\frac{32}{9}(1+\nu_r)^2+\frac{40}{9}(1+\nu_r)+\frac{8}{3}+\frac{1}{(1-\nu_r)}\left[\frac{(1+\nu_r)^4}{4}+2(1+\nu_r)^3+8(1+\nu_r)^2+16(1+\nu_r)+16\right]\right\}$
	Movable	$\frac{4\pi E_r h^3}{3(3+\nu_r)(1-\nu_r)a^2}$	$\frac{\pi E_r h}{a^2(3+\nu_r)^4}\left[\frac{191}{648}(1+\nu_r)^4+\frac{41}{27}(1+\nu_r)^3+\frac{32}{9}(1+\nu_r)^2+\frac{40}{9}(1+\nu_r)+\frac{8}{3}\right]$

*From reference 13.
**Derived using Babuno-Galerkin variational method, as reported in reference 13.

Table 2. Material Properties

Properties	Steel	Aluminum	Graphite/Epoxy (T300/5208)
E_r, GPa	199.95	68.95	50.81
E_z, GPa	199.95	68.95	11.78
G_r, GPa	75.17	25.92	19.38
G_{zr}, GPa	75.17	25.92	4.11
ν_r	0.33	0.33	0.31
ν_{zr}	0.33	0.33	0.06
ρ, density, kg/m^3	7971.8	2768.0	1611

*Quasi-isotropic laminate

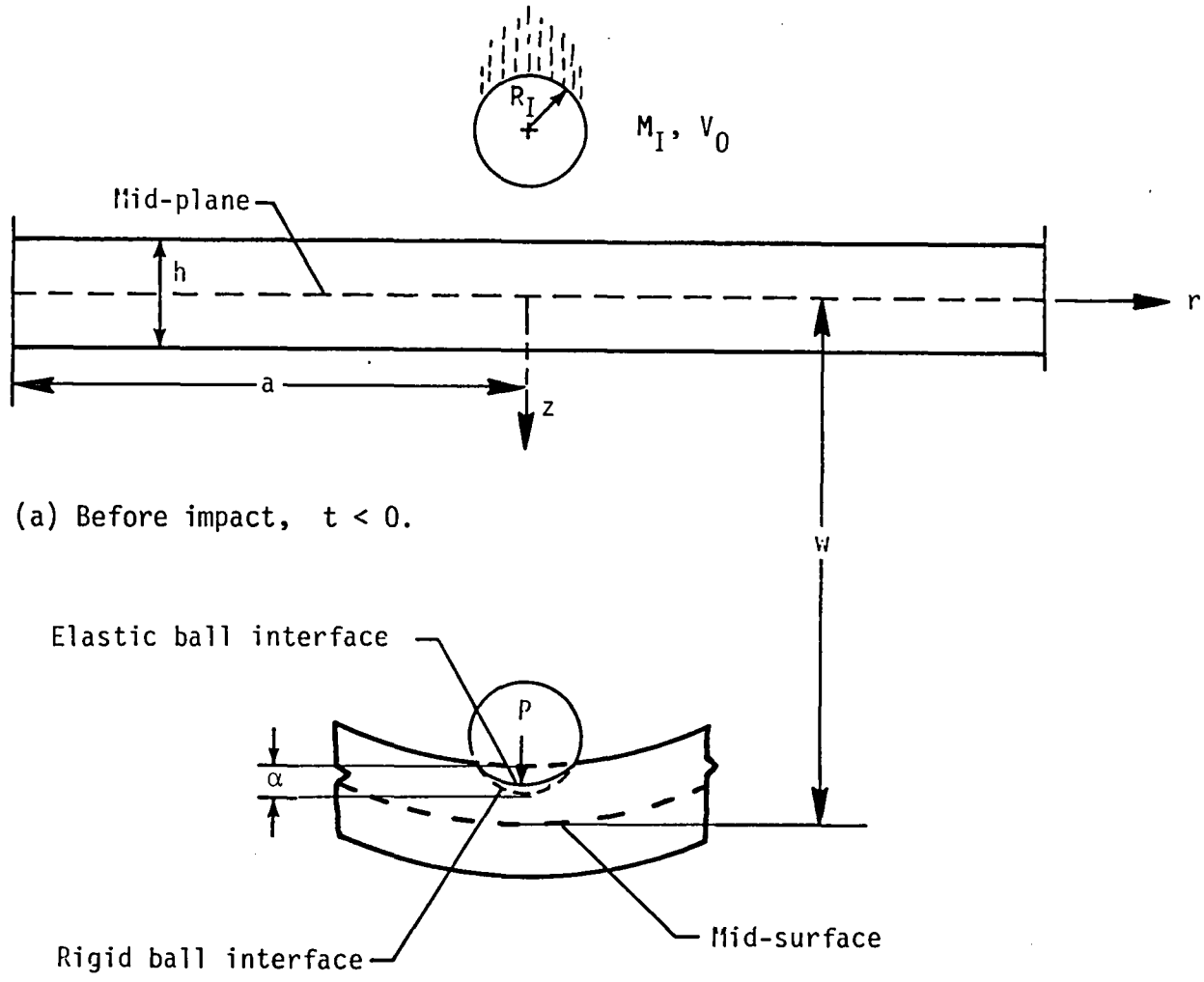

Figure 1.- Central transverse impact on a circular plate.

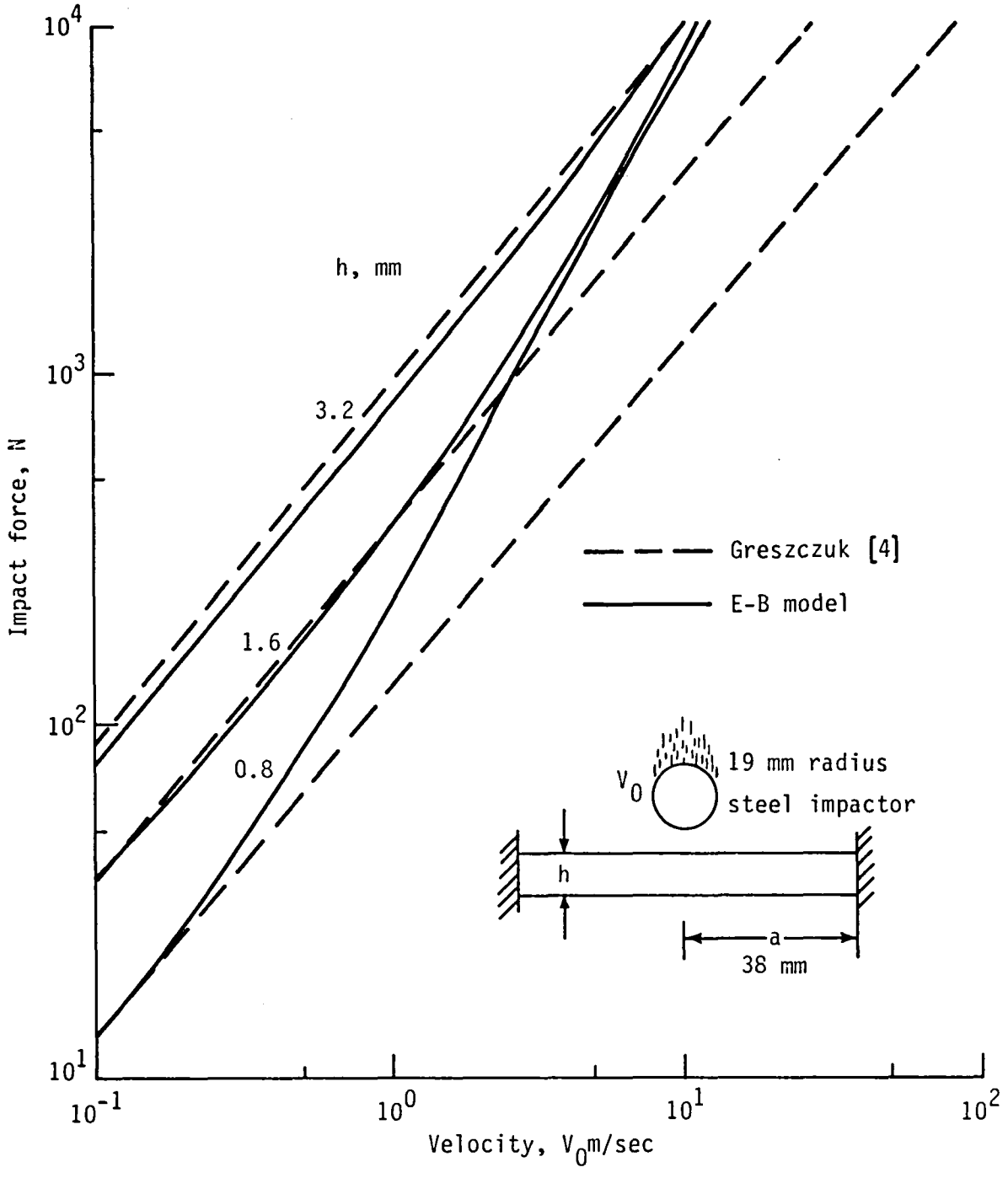

Figure 2.- Predicted impact force for clamped (immovable support) composite plates. (Graphite/epoxy quasi-isotropic laminate)

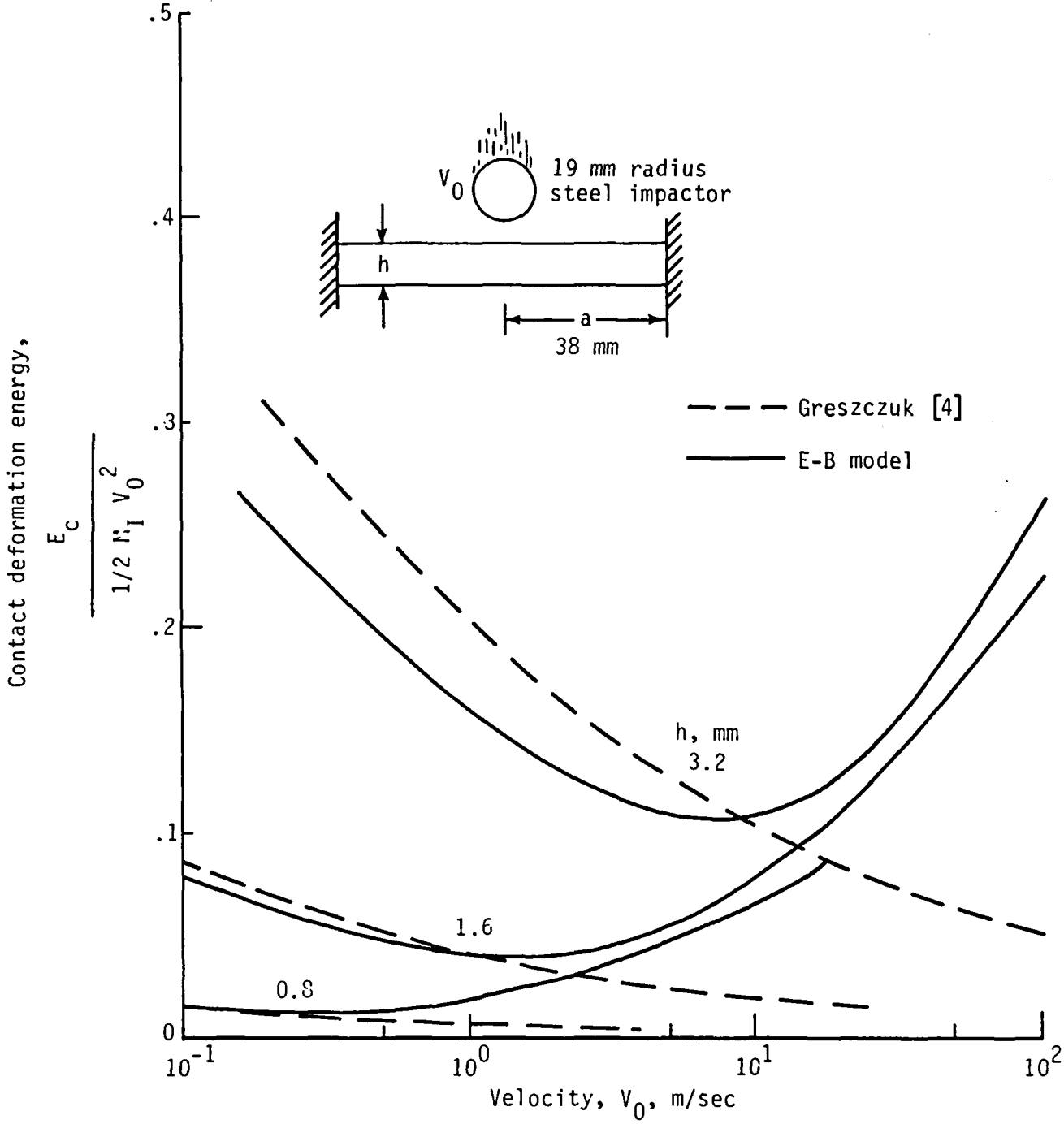

Figure 3.- Predicted contact energy ratio for clamped composite plate.
(Graphite/epoxy quasi-isotropic laminate)

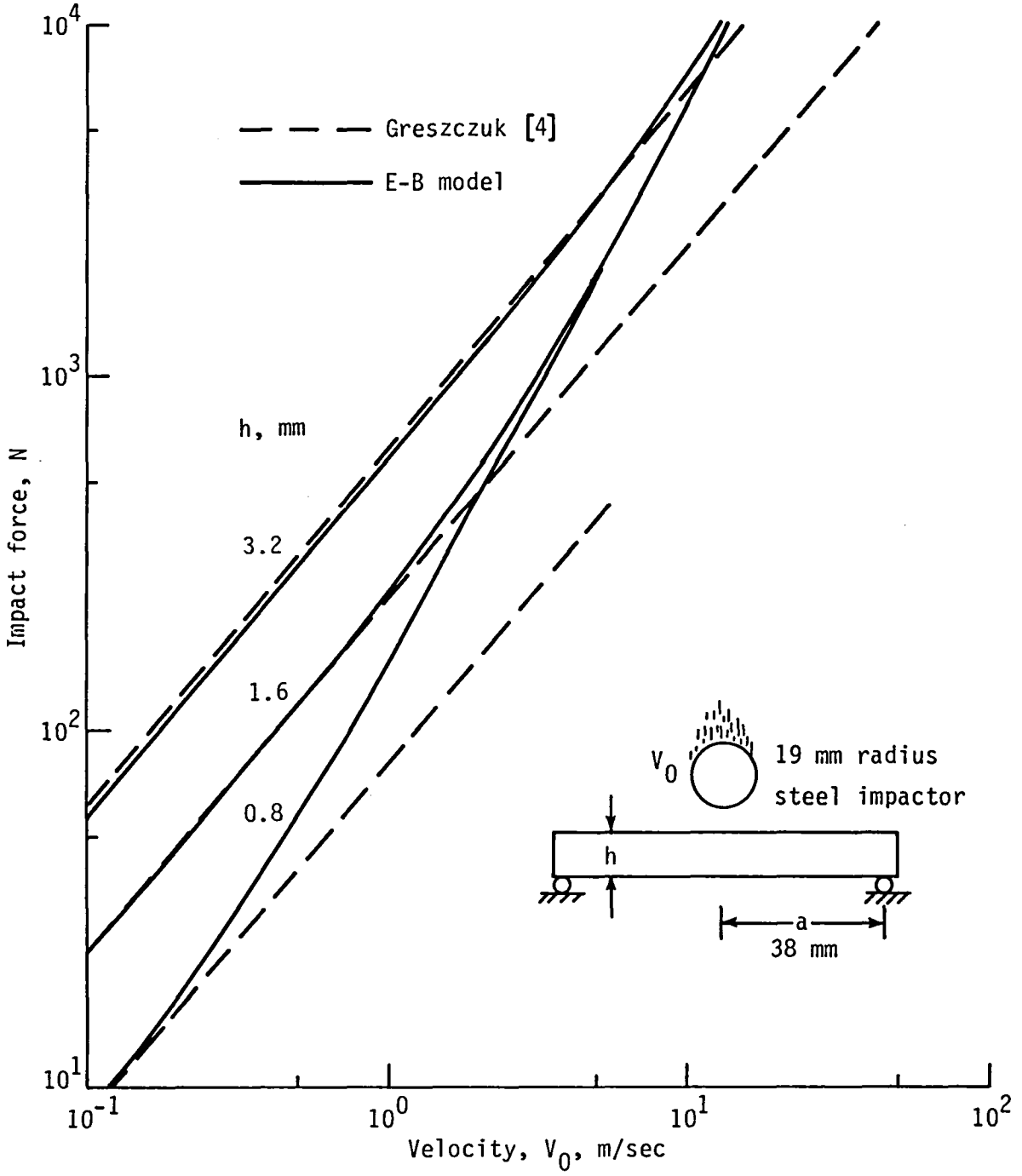

Figure 4.- Predicted impact force for simply-supported plates. (Graphite/epoxy quasi-isotropic laminate)

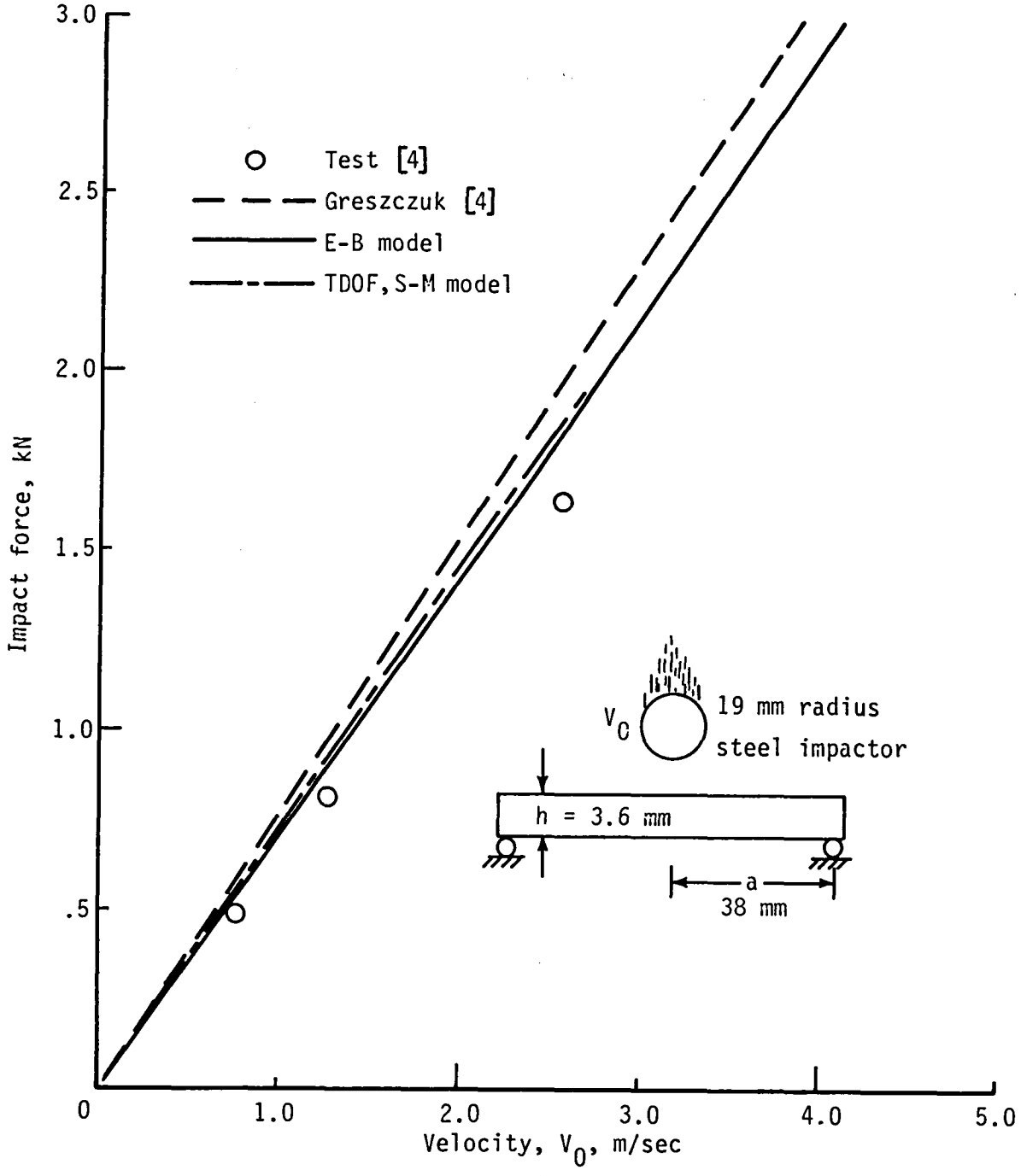

Figure 5.- Test-analyses comparison of impact force versus impact velocity for a simply-supported plate. (Graphite/epoxy quasi-isotropic laminate)

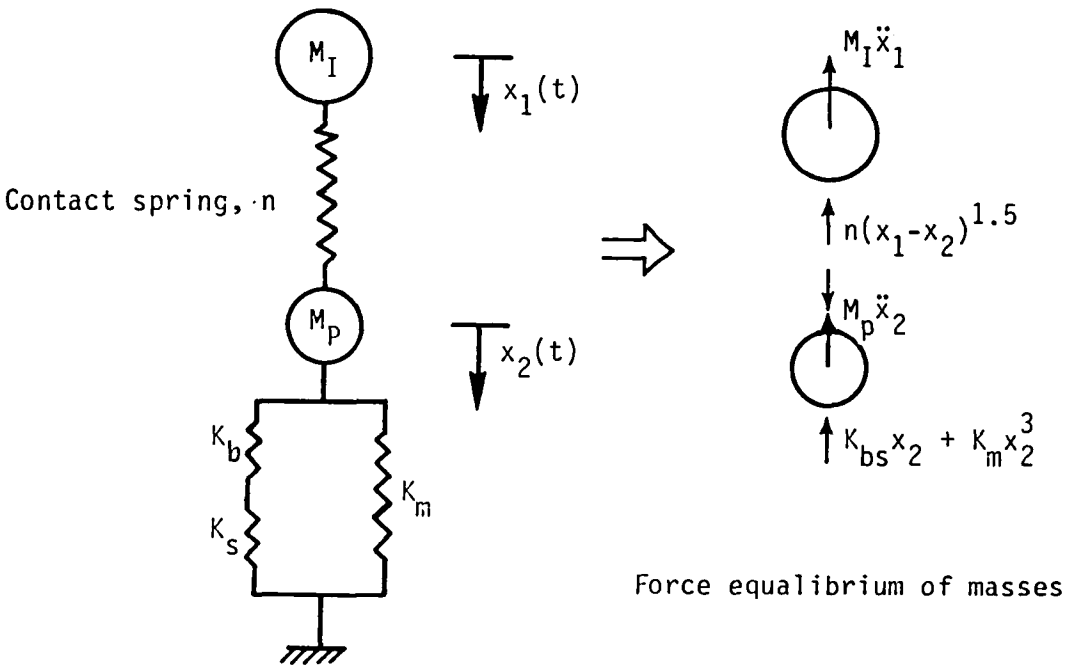

(a) Two degree-of-freedom spring-mass model.

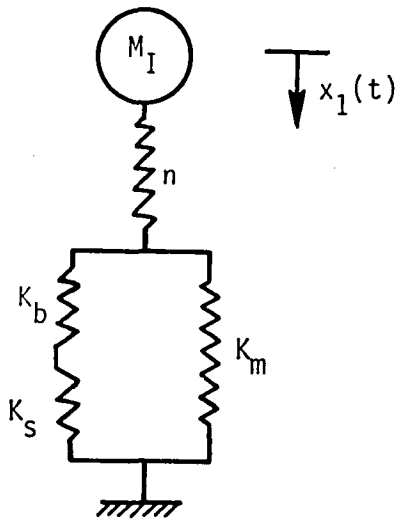

(b) Single degree-of-freedom spring-mass model.

Figure 6.- Spring-mass models for low-velocity impact of a circular plate.

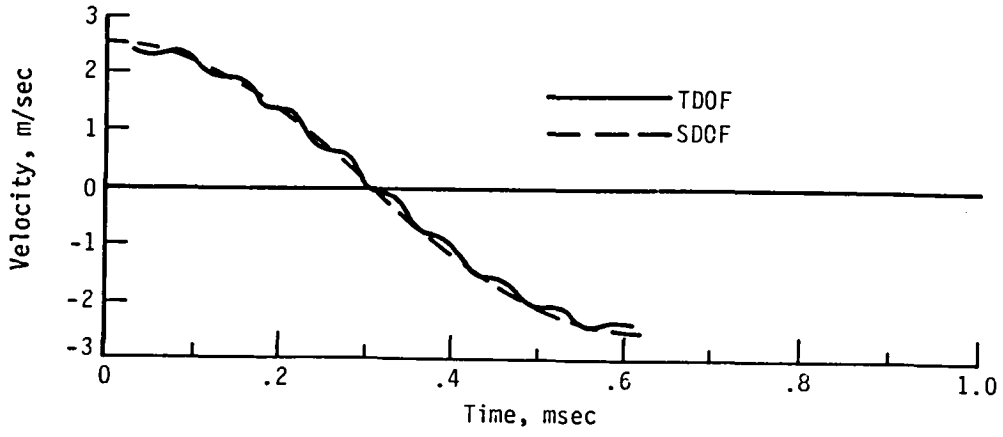

(a) Velocity response of the impactor.

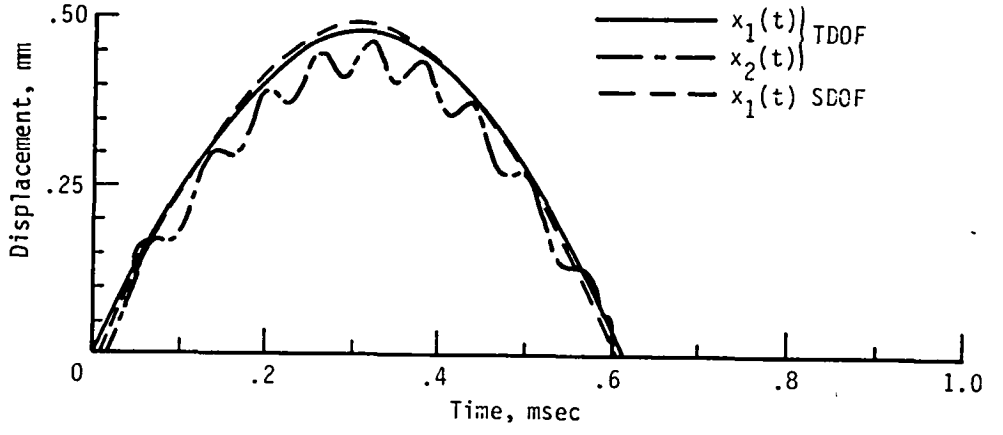

(b) Displacement response of the impactor and the plate.

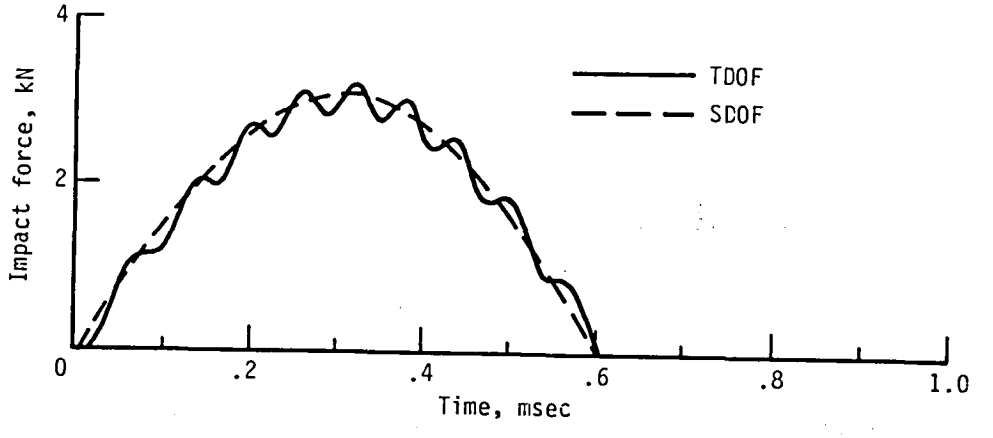

(c) Impact force response.

Figure 7.- Impact response of an aluminum plate using spring-mass models. (a = 38 mm, h = 3.2 mm, steel impactor, R_I = 19 mm)

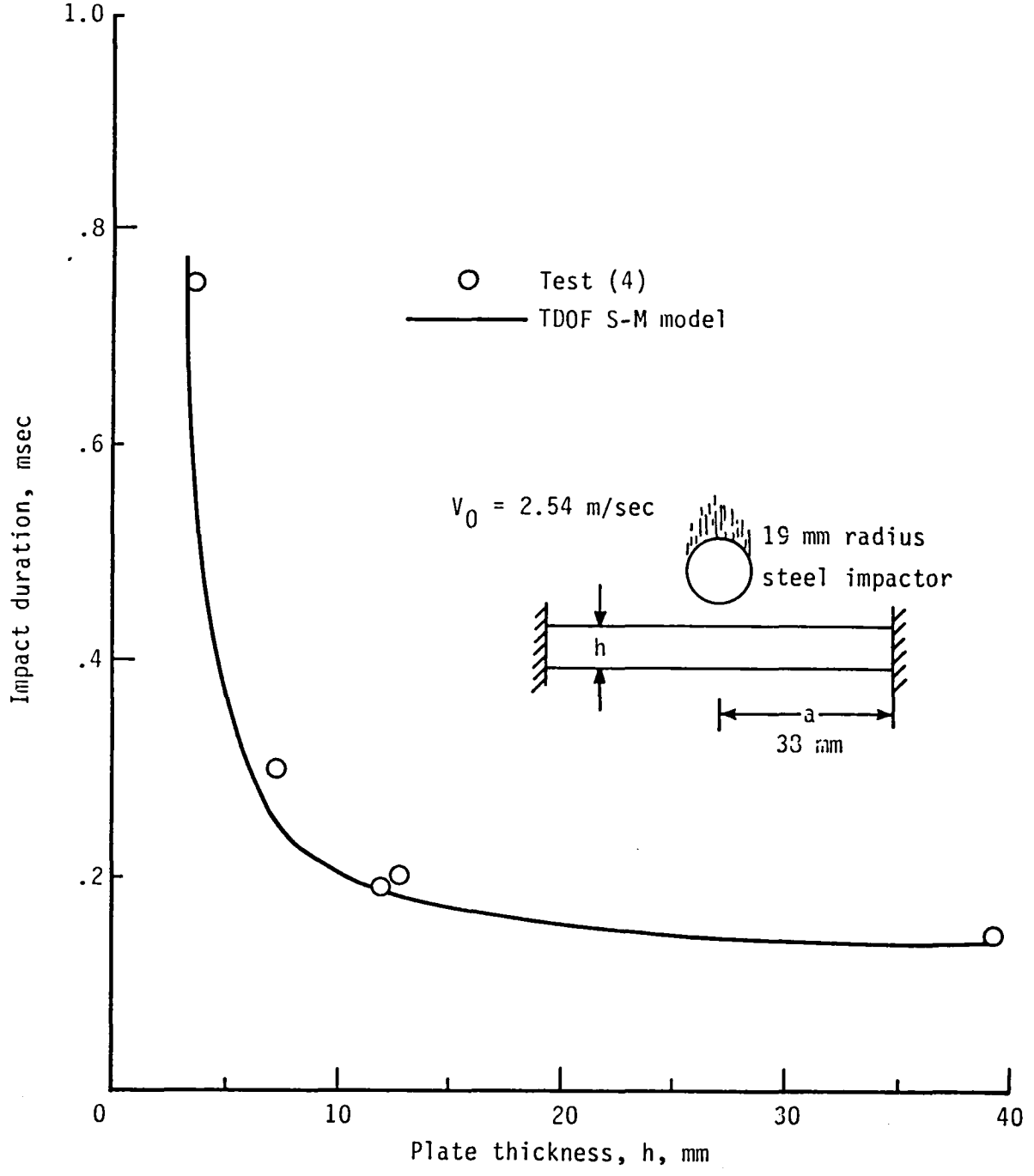

Figure 8.- Influence of plate thickness on impact duration for an aluminum plate.

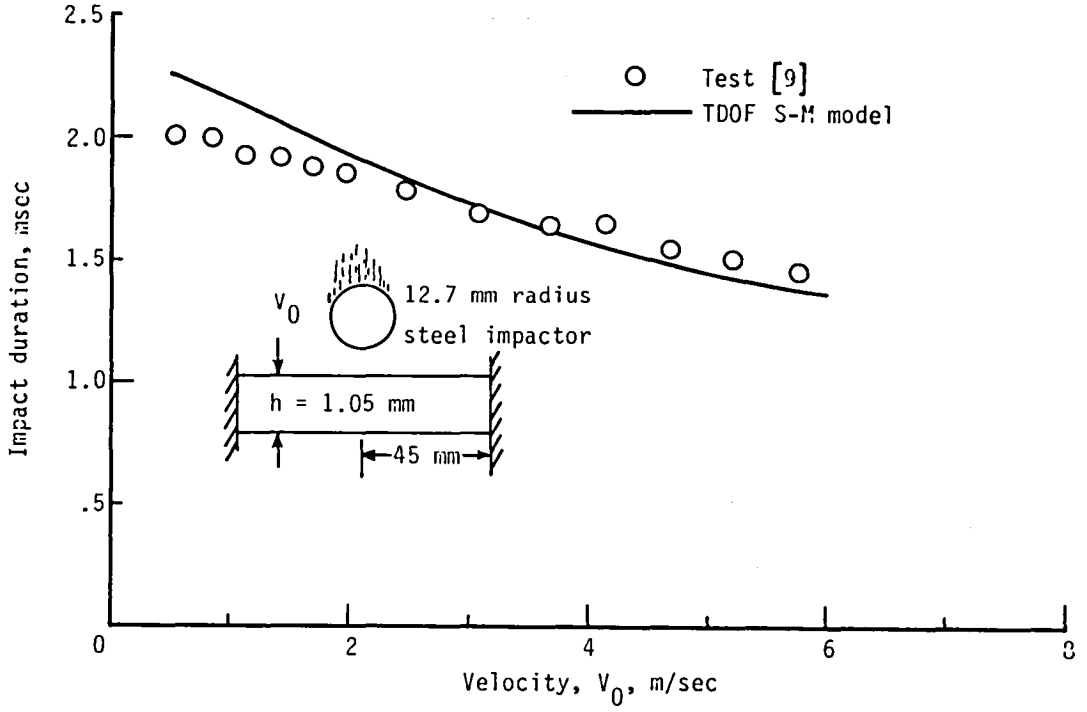

(a) Predicted and measured impact duration.

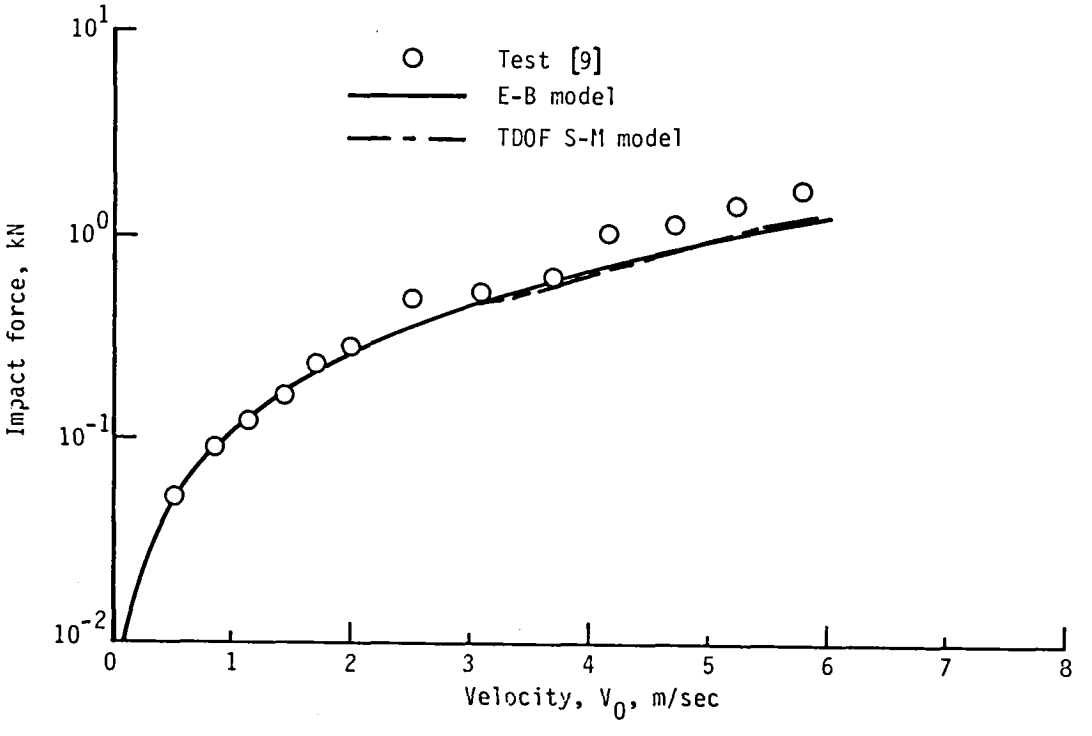

(b) Predicted and measured impact force.

Figure 9.- Impact on a clamped graphite/epoxy quasi-isotropic laminate.

1. Report No.	2. Government Accession No.	3. Recipient's Catalog No.
NASA TM-85703		

4. Title and Subtitle	5. Report Date
PREDICTION OF IMPACT FORCE AND DURATION DURING LOW VELOCITY IMPACT ON CIRCULAR COMPOSITE LAMINATES	October 1983
	6. Performing Organization Code: 506-53-23-05
7. Author(s): K. N. Shivakumar, W. Elber, and W. Illg	8. Performing Organization Report No.
	10. Work Unit No.
9. Performing Organization Name and Address: NASA Langley Research Center, Hampton, VA 23665	11. Contract or Grant No.
	13. Type of Report and Period Covered: Technical Memorandum
12. Sponsoring Agency Name and Address: National Aeronautics and Space Administration, Washington, DC 20546	14. Sponsoring Agency Code

15. Supplementary Notes

16. Abstract

Two simple and improved models--energy-balance and spring-mass--were developed to calculate impact force and duration during low-velocity impact of circular composite plates. Both models include the contact deformation of the plate and the impactor as well as bending, transverse shear, and membrane deformations of the plate. The plate was a transversely isotropic graphite/epoxy composite laminate and the impactor was a steel sphere. Calculated impact forces from the two analyses agreed with each other. The analyses were verified by comparing the results with reported test data.

17. Key Words (Suggested by Author(s))	18. Distribution Statement
Composite material Circular plate Energy-balance model Impact force Impact duration Spring-mass model	Unclassified - Unlimited Subject Category 24

19. Security Classif. (of this report)	20. Security Classif. (of this page)	21. No. of Pages	22. Price*
Unclassified	Unclassified	32	A03

* For sale by the National Technical Information Service, Springfield, Virginia 22161